Applied Catalysis B: Environmental 94 (2010) 179–185

Contents lists available at ScienceDirect

Applied Catalysis B: Environmental

journal homepage: www.elsevier.com/locate/apcatb

# Tailored activated carbons as catalysts in biodecolourisation of textile azo dyes

Gergo Mezohegyi [a], Filomena Gonçalves [b], José J.M. Órfão [b], Azael Fabregat [a,*], Agustí Fortuny [c], Josep Font [a], Christophe Bengoa [a], Frank Stuber [a]

[a] Departament d'Enginyeria Química, ETSEQ, Universitat Rovira i Virgili, Av. Països Catalans 26, 43007 Tarragona, Catalunya, Spain
[b] Laboratório de Catálise e Materiais (LCM), Laboratório Associado LSRE/LCM, Departamento de Engenharia Química, Faculdade de Engenharia, Universidade do Porto, Rua Dr. Roberto Frias, 4200-465 Porto, Portugal
[c] Departament d'Enginyeria Química, EPSEVG, Universitat Politécnica de Catalunya, Av. Víctor Balaguer s/n, 08800 Vilanova i la Geltrú, Catalunya, Spain

ARTICLE INFO

*Article history:*
Received 21 August 2009
Received in revised form 1 November 2009
Accepted 7 November 2009
Available online 11 November 2009

*Keywords:*
Azo dye
Reduction
Activated carbon
Packed-bed reactor
Surface chemistry

ABSTRACT

Anaerobic reduction of two textile azo dyes (Orange II and Reactive Black 5) was investigated in upflow stirred packed-bed reactors (USPBRs) with biological activated carbon (BAC) system. The bioreactors were prepared with tailored activated carbons (ACs) having different textural properties and various surface chemistries. A kinetic model proposed previously was able to describe the catalytic azo reduction in all cases. Decolourisation with very high reduction rates took place in the case of each AC. Best dye removals were ensured by the AC having the highest surface area: conversion values above 88% were achieved in the case of both azo dyes at a space time of 0.23 min or higher, corresponding to a very short hydraulic residence time of about 0.30 min at the most. The decolourisation rates were found to be significantly influenced by the textural properties of AC and moderately affected by its surface chemistry. The results confirmed the catalytic effects of carbonyl/quinone sites and, in addition, delocalized π-electrons seemed to play a role in the catalytic reduction in the absence of surface oxygen groups.



## 1. Introduction

Textile industry is one of those industries that consume large amounts of water in the manufacturing process [1] and, also, discharge great amounts of effluents with synthetic dyes to the environment causing public concern and legislation problems. Azo dyes, that make up the majority (60–70%) of the dyes applied in textile processing industries [2] are considered to be serious health-risk factors. Apart from the aesthetic deterioration of water bodies, many azo colourants and their breakdown products are toxic to aquatic life [3] and can cause harmful effects to humans [4,5]. Several physico-chemical and biological methods for dye removal from wastewater have been investigated [6–9] and seems that each technique faces the facts of technical and economical limitations [8]. However, microbial decolourisation of dyes [8,10–12] is one of the most attractive technologies considering its economic, environmentally suitable and methodologically relatively simple features.

Azo dyes are xenobiotic compounds and due to their electron withdrawing nature, they tend to persist under aerobic environment [13]. However, under anaerobic conditions, decolourisation is achieved while the aromatic amines produced from such azo cleavage can be removed aerobically [14]. These predicted the efficacy of an anaerobic–aerobic reactor sequence for complete azo dye treatment [14,15]. The most serious drawback of azo dye reduction by bacteria used to be the slowness of the process. A few study have cleared that certain electron mediators such as quinone-like compounds can greatly accelerate decolourisation rates in homogeneous reactions [2,16,17]. On the other hand, heterogeneously catalyzed azo bioreduction by a solid redox mediator such as activated carbon (AC), has been reported to be a very promising process [18–21].

In catalysis, ACs have been mainly used as support, but their use as catalysts on their own is growing quickly [22–26]. One of the advantages of ACs is the possibility of tailoring their physical and/or chemical properties in order to optimise their performance for specific applications [27]. This means that both their pore structure and surface chemistry can be varied [27–29] to meet the demands of the catalytic reaction considered. In textile and dye wastewater treatments, the role of activated carbon has been often limited to dye adsorption. If AC is considered as a catalyst in biological azo dye decolourisation, its specific modification may increase dye removal rates. In the present study, several activated carbons with modified pore structures or surface chemistries were applied for the first time in anaerobic upflow stirred packed-bed reactors [20] for azo dye reduction, and the effects of AC texture and surface chemical group variation on decolourisation rates were discussed.

* Corresponding author. Tel.: +34 977 559643; fax: +34 977 559667.
*E-mail address:* afabrega@urv.cat (A. Fabregat).

0926-3373/$ – see front matter © 2009 Elsevier B.V. All rights reserved.
doi:10.1016/j.apcatb.2009.11.007

## 2. Experimental

### 2.1. Preparation of activated carbons

#### 2.1.1. Activated carbons with different textural properties

The initial material selected (sample $AC_0$) was the commercial activated carbon Norit Rox 0.8, which was supplied in the form of cylindrical pellets of 0.8 mm diameter and 5 mm length. The activated carbons with larger porosities were obtained by $CO_2$ gasification of sample $AC_0$ previously impregnated with 3.5% of cobalt. The role of cobalt was to catalyze the gasification of carbon, thereby promoting the formation of mesopores [27]. The impregnation was carried out by mixing the previously vacuum-degassed sample $AC_0$ with an aqueous solution of $Co(NO_3)_2{\cdot}6H_2O$. The resulting suspension was shaken for 2 h. Then the sample was washed with distilled water and dried at 100 °C overnight in an oven.

The gasification experiments were carried out in a tubular vertical reactor under the following experimental conditions: heating from room temperature to 900 °C at 10 °C $min^{-1}$ under a flow of 100 $cm^3$ $min^{-1}$ of $N_2$; at 900 °C the gas was changed to $CO_2$ maintaining the flow rate and the sample was gasified during 40 min ($AC_{T1}$) or 120 min ($AC_{T2}$) and finally cooled down to room temperature under a flow of 100 $cm^3$ $min^{-1}$ of $N_2$. These carbons were subsequently washed with a 2 M HCl-solution to remove cobalt, followed by washing with distilled water until reaching neutral pH and dried in the oven at 100 °C. To make comparison with the starting carbon possible, $AC_0$ was also heated up to 900 °C and was kept at this temperature for 40 min under a flow of 100 $cm^3$ $min^{-1}$ of $N_2$ ($AC_{T0}$) to ensure similar surface chemistry to the gasificated samples. Since the quinonic surface groups are supposed to play an important role during anaerobic biodecolourisation of azo dyes by biological activated carbon, and a significant amount of these groups were removed by the heat treatment, a slight oxidation was applied for samples $AC_{T0}$, $AC_{T1}$ and $AC_{T2}$. These carbons were heated up to 425 °C at 10 °C $min^{-1}$ under a flow of 75 $cm^3$ $min^{-1}$ of $N_2$; when the given temperature was reached, air was added to the gas flow to have 5% (v/v) of $O_2$; this gaseous mixture was passed for 4 h. When cooling started, the gas was set back only to $N_2$. After cooling to room temperature, all the carbon samples were crushed and granules of 25–50 mesh size (0.7–0.3 mm) were separated and stored under normal conditions.

#### 2.1.2. Activated carbons with different surface chemistries

The treatments outlined below were carried out in order to obtain materials with different surface chemistries, while maintaining the original textural properties as far as possible.

Liquid-phase oxidation of $AC_0$ with $HNO_3$ was performed using a 250 $cm^3$ Soxhlet extraction apparatus. Initially, 400 $cm^3$ of 5 M $HNO_3$ were introduced into a 500 $cm^3$ Pyrex round bottom flask and heated to boiling temperature with a heating mantle. The Soxhlet with a certain amount of activated carbon was connected to the boiling flask and to the condenser. The reflux was stopped after 6 h. The AC was then washed with distilled water to neutral pH and dried in an air convection oven at 100 °C for 24 h (sample $AC_1$).

Sequentially, the sample $AC_1$ was altered by thermal treatments; the starting material had to present a large amount of surface groups that were to be removed in different amounts (and types) by applying different temperatures. In every case, 3 g of sample $AC_1$ were placed into a fused silica tubular reactor. The heating was done under a flow of $N_2$ at 100 $cm^3$ $min^{-1}$ and the heating rate was 10 °C $min^{-1}$. The carbon samples were heated up to 400 °C ($AC_2$), 600 °C ($AC_3$), 750 °C ($AC_4$) and 1100 °C ($AC_5$). $AC_5$ was kept at 1100 °C for 1 h. Posteriorly, one additional sample was prepared from $AC_0$ by heating it up to 750 °C under a flow of $N_2$ at 100 $cm^3$ $min^{-1}$ and heating rate of 10 °C $min^{-1}$ ($AC_{02}$). After cooling to room temperature under the same atmosphere, all the carbon samples were crushed and granules of 25–50 mesh size (0.3–0.7 mm) were separated and stored under normal conditions.

### 2.2. Characterization of activated carbons

#### 2.2.1. Textural characterization

The textural characterization of the materials was principally important in the case of pore size-modified activated carbons, but it was also checked if there had been notable textural changes after the surface chemistry modifications, including the thermal treatments. This characterization was based on the $N_2$ adsorption isotherms, determined at 77 K with a Coulter Omnisorp 100 CX gas adsorption analyser. The micropore volume ($V_\mu$) and the non-microporous surface area ($S_{\neq\mu}$) were calculated by the *t*-method, using the standard isotherms for carbon materials proposed by Rodriguez-Reinoso et al. [30]. The BET surface areas ($S_{BET}$) of the samples were also calculated for comparison purposes.

#### 2.2.2. Surface chemistry characterization

The temperature-programmed desorption (TPD) profiles of the samples were obtained in an Altamira AMI-200 characterization unit, working with a U-shaped tubular microreactor, placed inside an electrical furnace. The flow of the helium carrier gas was 25 $cm^3$ $min^{-1}$, the temperature was programmed to linearly rise up to 1100 °C at a heating rate of 5 °C $min^{-1}$. The amounts of CO and $CO_2$ desorbed from the carbon samples (100 mg) were determined by an Ametek Dymaxion mass spectrometer. The relative molecular masses monitored for all samples were 2 ($H_2$), 16 (O), 18 ($H_2O$), 28 (CO) and 44 ($CO_2$).

The determination of $pH_{PZC}$ (point of zero charge) of the samples was similarly carried out as reported by Órfão et al. [31]: 20 $cm^3$ of 0.01 M NaCl solution was placed in a closed Erlenmayer flask. The pH was adjusted to a value between 2 and 10 by adding HCl 0.1 M or NaOH 0.1 M solutions. Then, 0.05 g of each sample was added and the final pH measured after 48 h under agitation at room temperature. The $pH_{PZC}$ is the point where the curve $pH_{final}$ vs. $pH_{initial}$ crosses the line $pH_{initial} = pH_{final}$. Blank tests without carbon were also made in order to eliminate the influence of $CO_2$ from air on pH.

### 2.3. Chemicals

Azo dyes Orange II sodium salt (dye content 93%, Sigma, ref. O8126) and Reactive Black 5 (55%, Sigma–Aldrich, ref. 306452) were selected as model textile dyes. In order to simulate dye-bath effluents from dyeing processes with azo reactive dyes, hydrolysis of Reactive Black (RB5H) was accomplished by: dissolving it in distilled water, adjusting the pH to 12.0 with 1 M NaOH, boiling for 2 h, cooling the solution down, setting the pH to 7.0 with 1 M/0.1 M HCl and adjusting the necessary volume of prepared stock solution with distilled water. Sodium acetate (99%, Aldrich, ref. 11019-1) was used as co-substrate being both the carbon source for microorganisms and electron donor for azo reduction. The basal media contains several compounds (mg $L^{-1}$): $MnSO_4{\cdot}H_2O$ (0.155), $CuSO_4{\cdot}5H_2O$ (0.285), $ZnSO_4{\cdot}7H_2O$ (0.46), $CoCl_2{\cdot}6H_2O$ (0.26), $(NH4)_6Mo_7O_{24}$ (0.285), $MgSO_4{\cdot}7H_2O$ (15.2), $CaCl_2$ (13.48), $FeCl_3{\cdot}6H_2O$ (29.06), $NH_4Cl$ (190.9), $KH_2PO_4$ (8.5), $Na_2HPO_4{\cdot}2H_2O$ (33.4), and $K_2HPO_4$ (21.75).

### 2.4. Feed and bioreactor system

The upflow stirred packed-bed reactor (USPBR) system and operating parameters used in this study were similar to those

described in a former study of the authors [20]. The reduction of dyes was tested in reactors containing 1 g of activated carbon with the immobilized microorganisms (Fig. 1) originated from a non-specific anaerobic mixed culture [19]. The reactor had a diameter of 15 mm with a useful volume of about 2 $cm^3$. The packed-bed porosity was about 0.3. Two filters, placed into the top and bottom of the reactor, prevented washing out of the carbon. The temperature was kept constant at 35 °C. The entering concentration of dyes was 100 mg $L^{-1}$. The feed also contained 200 mg $L^{-1}$ of sodium acetate and the basal media with microelements. The flow rate of the feed was varied between 25 and 250 mL $h^{-1}$ and was ensured by a micro pump (Bio-chem Valve Inc., ref. 120SP2420-4TV). The anaerobic condition in the feeding bottle (5 L) was maintained by both cooling of the solution (at 5 °C) and bubbling of helium. The redox potential was continuously monitored and remained below −500 mV (referred to a combined Pt//Ag/AgCl redox electrode). Agitation of the biomass was applied for 1 h/day and sampling was done immediately after or during this period. Before starting experiments in USPBRs, the activated carbon bed was saturated with the azo dyes at 100 mg $L^{-1}$ concentration to avoid the influence of initial dye adsorption during the initial period of operation.

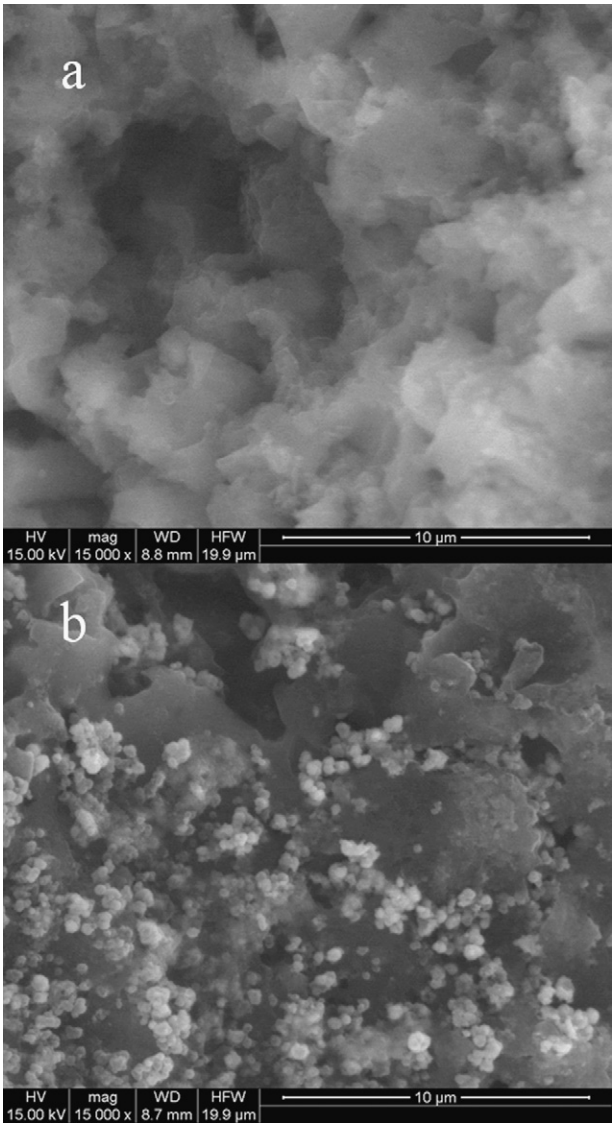


**Fig. 1.** Activated carbon surface without (a) and with (b) biofilm (ESEM).

### 2.5. Analytical methods

Both dyes and the monoazo reduction product of RB5H ($RB5H_M$) were measured by HPLC on a $C_{18}$ Hypersil ODS column. A gradient of methanol–water (M:W) mobile phase was applied (M:W solvent ratios (%) were: 45:55 for RB5H and 70:30 for OII). OII, RB5H and $RB5H_M$ were determined at 487, 597 and 530 nm, respectively.

## 3. Results and discussion

### 3.1. Characterization of activated carbons

#### 3.1.1. Textural characterization

Fig. 2 shows the $N_2$ adsorption isotherms for the activated carbon samples after textural (Fig. 2a) and surface chemistry modification (Fig. 2b). The shape of the isotherms denotes the presence of micropores but mainly the mesopores in the carbon samples. The textural modification of AC resulted in the enhancement of the porosity. Evidently, the longer time of gasification was applied, the higher burn-off values were reached (28% and 50% for $AC_{T1}$ and $AC_{T2}$, respectively). Some calculated data confirms these observations and shows that the gasification time correlates to several textural factors (Table 1). On the other hand, surface chemistry modification by acid and consecutive thermal treatment of $AC_0$ did not cause significant textural changes, only a very slight reduction of microporosity was observed while the meso- and

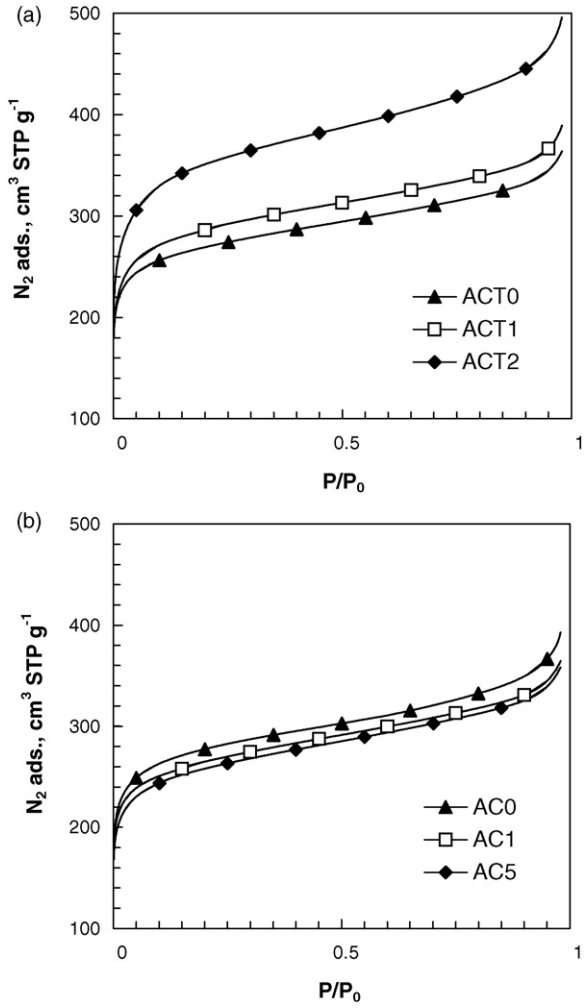


**Fig. 2.** $N_2$ adsorption isotherms at 77 K for activated carbons with different textural properties (a) and surface chemistries (b).

**Table 1**
Textural data of selected activated carbons used in this study.

| Carbon | [a]$S_{BET}$ ($m^2 g^{-1}$) | [b]$V_{\mu}$ ($cm^3 g^{-1}$) | [c]$S_{\neq\mu}$ ($m^2 g^{-1}$) |
|---|---|---|---|
| $AC_0$ | 1055 | 0.415 | 90 |
| $AC_1$ | 1004 | 0.409 | 75 |
| $AC_5$ | 977 | 0.401 | 76 |
| $AC_{T0}$ | 1027 | 0.417 | 71 |
| $AC_{T1}$ | 1097 | 0.444 | 74 |
| $AC_{T2}$ | 1336 | 0.534 | 113 |

[a] BET surface area.
[b] Microporous volume.
[c] Non-microporous surface area.

macroporosity remained intact; thus a possible variation in biodecolourisation rates with these carbons would be solely due to their different surface chemistries.

### 3.1.2. Surface chemistry characterization

The surface oxygen groups on carbon materials decompose upon heating by releasing CO and $CO_2$ at different temperatures. A $CO_2$ peak results from carboxylic acids at low temperatures, or lactones at higher temperatures; carboxylic anhydrides originate both a CO and a $CO_2$ peak; phenols, ethers, and carbonyls/quinones originate CO peaks [28]. Fig. 3 shows the TPD spectra of the Norit Rox activated carbon before ($AC_0$) and after the textural modifications. Because of their preparation method, none of these carbon samples ($AC_{T0}$, $AC_{T1}$ and $AC_{T2}$) contains significant amount

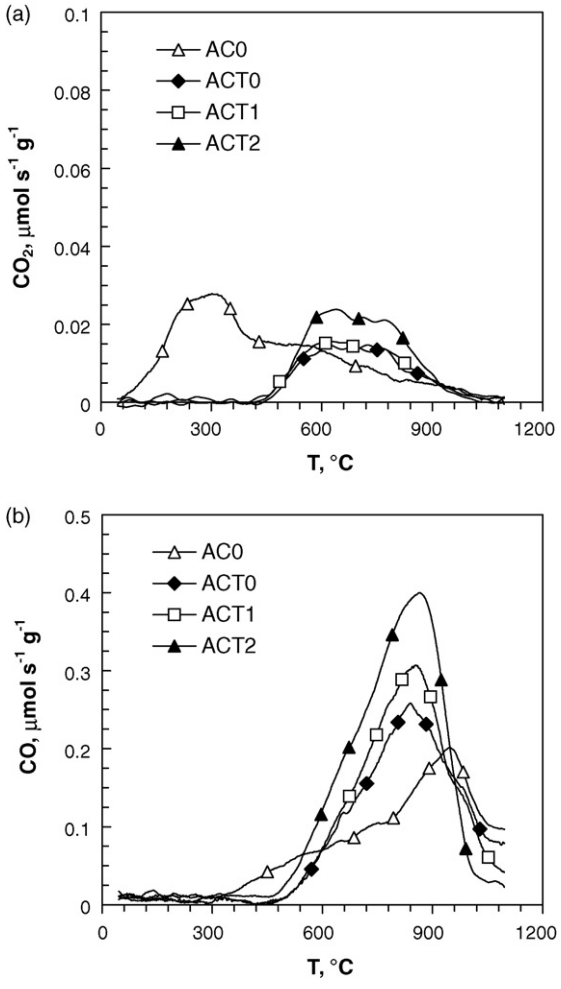


**Fig. 3.** TPD spectra of activated carbons with different textural properties: (a) $CO_2$ and (b) CO evolution.

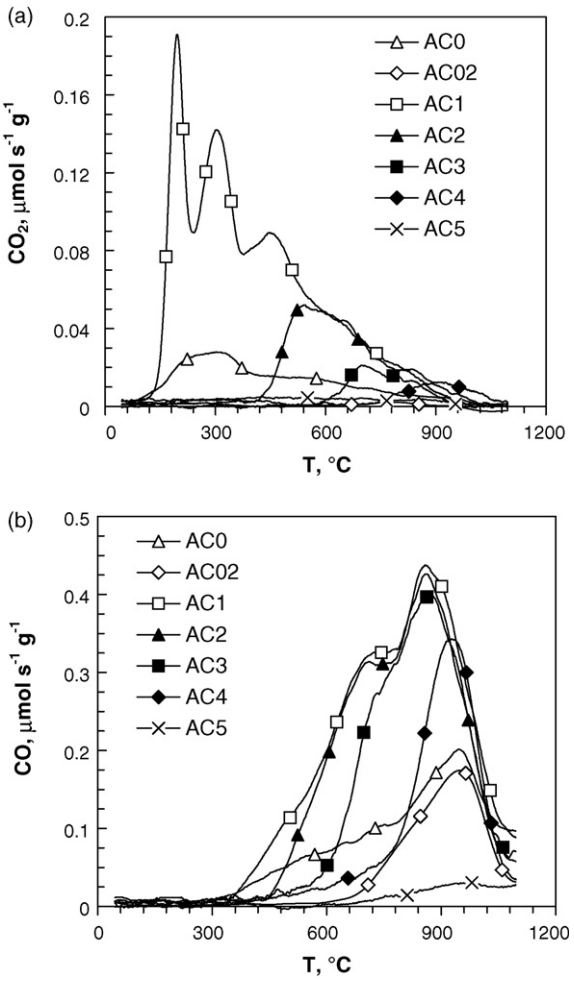


**Fig. 4.** TPD spectra of activated carbons with different surface chemistries: (a) $CO_2$ and (b) CO evolution.

of surface groups emitting $CO_2$ (Fig. 3a), its rate of generation was less than 0.03 μmol $s^{-1}$ $g^{-1}$ in each case. The amount of CO-emitting groups is obviously higher by the increase of the activated carbon surface area (Fig. 3b), but the specific CO-releasing groups density was found to be similar for $AC_{T0}$, $AC_{T1}$ and $AC_{T2}$ (1.00, 1.04 and 1.08 μmol $m^{-2}$, respectively). According to both the CO- and $CO_2$-spectra, the textural modification (followed by slight oxidation) was carried out by varying mainly the textural characteristics but not the surface chemistries of the carbon samples ($AC_{T0}$, $AC_{T1}$ and $AC_{T2}$).

Fig. 4 shows the TPD spectra of $AC_0$ and the samples with modified surface chemistries ($AC_1$–$AC_5$; $AC_{02}$). It can be seen that the nitric acid treatment ($AC_1$) increased the amount of surface groups, which is evidenced by the increase of $CO_2$ (Fig. 4a) and CO (Fig. 4b) released. Both the spectra show well the effect of thermal treatments on sample $AC_1$; the higher temperature was applied, the more amount of surface groups were removed. In case of thermal treatment at 1100 °C ($AC_5$), no significant amount of surface groups remained on the carbon. Table 2 shows the total amounts of CO and $CO_2$ released, obtained by integration of the areas under the TPD peaks, the ratio $CO/CO_2$ and the point of zero charge of the samples with different surface chemistries. A good correlation was found between the BET surface areas and the evolved amounts of CO and $CO_2$ in the case of texture-modified samples, as mentioned before.

In order to determine the amount of individual surface groups, the deconvolution of the CO- and $CO_2$-spectra was carried out for

**Table 2**
Surface chemistry data of activated carbon samples.

| Sample | $CO_2$ ($\mu$mol g$^{-1}$) | CO ($\mu$mol g$^{-1}$) | CO/$CO_2$ | $pH_{PZC}$ |
|---|---|---|---|---|
| $AC_0$ | 144 | 911 | 6.3 | 8.3 |
| $AC_{T0}$ | 62 | 1023 | 16.5 | n.m. |
| $AC_{T1}$ | 68 | 1136 | 16.7 | n.m. |
| $AC_{T2}$ | 94 | 1448 | 15.4 | n.m. |
| $AC_1$ | 628 | 2041 | 3.2 | 4.5 |
| $AC_2$ | 181 | 1808 | 10.0 | 7.3 |
| $AC_3$ | 51 | 1481 | 29.0 | 7.6 |
| $AC_4$ | 35 | 888 | 25.4 | 8.1 |
| $AC_5$ | n.d. | 106 | – | 8.6 |
| $AC_{02}$ | n.d. | 498 | – | n.m. |

n.m., not measured; n.d., not detectable.

all carbon samples, according to the numerical calculations described by Figueiredo et al. [32]. A multiple gaussian function was used for fitting each of the TPD spectra, taking the position of the peak center as initial estimate (Fig. 5). The numerical calculations were based on a non-linear routine which minimized the square of the deviations, using the Simplex method to perform the iterations. Table 3 gives the deconvolution data of the main peaks obtained, where $T_M$ is the temperature of the peak maximum and $A$ is the integrated peak area. According to the individual peak data, only the sample $AC_1$ contains significant amount of $CO_2$-releasing (acid and anhydride) groups on its surface, together with presenting the smallest CO:$CO_2$ ratio among all the carbon samples. The CO-emitting groups on each ACs are present in higher amounts and among them, carbonyl/quinone sites can be considered as the most significant ones.

The $pH_{PZC}$ values are consistent with the CO and $CO_2$ evolutions (Table 2). The $HNO_3$-treatment originated a large amount of oxygen-containing surface groups having mainly acid characteristics (sample $AC_1$). After thermal treatments at high temperatures (>700 °C), practically only CO-releasing groups remained on the carbon surface, which have neutral or basic properties. However, the basic characteristics associated with activated carbons submitted to thermal treatments are mainly associated with the electron-rich oxygen-free sites located on the carbon basal planes (Lewis basicity). Although $pH_{PZC}$ is considered to have serious significance in the adsorption of dyes onto activated carbons [33], probably it is not the crucial factor in the present biological reduction process, which is rather dependent on electrochemical characteristics of the system [21].

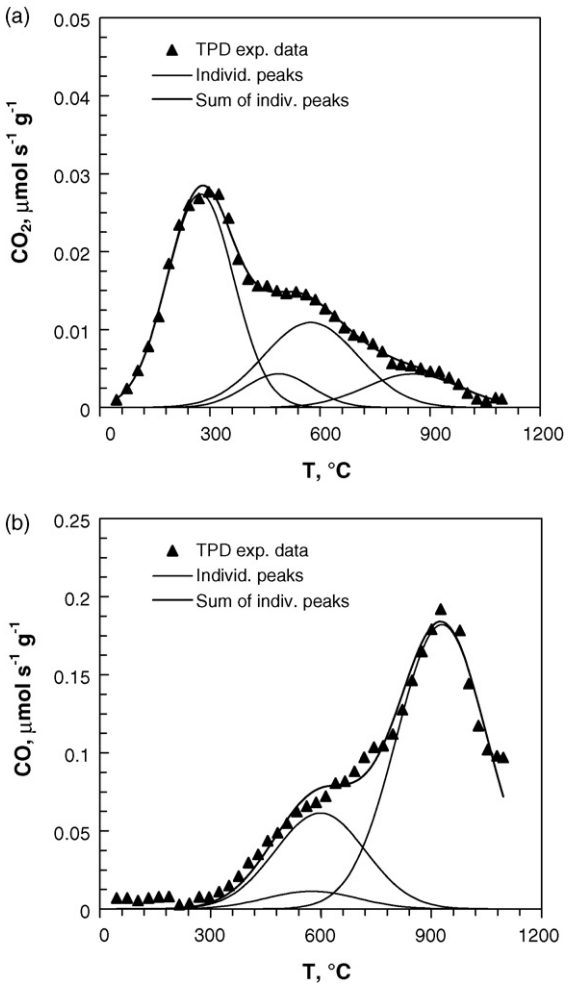


**Fig. 5.** Deconvolution of TPD spectra: example for (a) $CO_2$ and (b) CO evolution ($AC_0$).

### 3.2. Reduction of azo dyes

#### 3.2.1. Modeling

The efficacy of the anaerobic upflow stirred packed-bed reactor with biological activated carbon system for mono- and diazo reduction was proved in an earlier study of the authors [21]. The degradation model involving both heterogeneous catalysis and biological decolourisation with Michaelis–Menten-like kinetics can be given as:

$$\frac{dc_{DYE}}{\rho d\tau} = -\frac{k_1 c_{DYE}}{k_2 + c_{DYE}} \quad (1)$$

where $c_{DYE}$ (mmol L$^{-1}$) is the dye concentration, $\tau$ (min $g_{AC}$ g$^{-1}$) is the space time, $\rho$ (g L$^{-1}$) is the density of solution, and $k_1$ (mmol $g_{AC}^{-1}$ min$^{-1}$) and $k_2$ (mmol L$^{-1}$) are the kinetic parameters. In case of a diazo colourant (RB5H), the material balance equation for the monoazo reduction product is:

$$\frac{dc_{RB5HM}}{\rho d\tau} = \frac{k_1 c_{DYE}}{k_2 + c_{DYE}} - \frac{k_3 c_{RB5HM}}{k_4 + c_{RB5HM}} \quad (2)$$

where $c_{RB5HM}$ (mmol L$^{-1}$) is the monoazo product concentration and $k$ values ($k_3$: mmol $g_{AC}^{-1}$ min$^{-1}$ and $k_4$: mmol L$^{-1}$) are the referred kinetic constants. Eq. (2) can be easily solved numerically using for instance the Euler method.

#### 3.2.2. Catalytic reduction by ACs with different textural properties

Fig. 6 shows an example ($AC_0$) that the kinetic models Eqs. (1) and (2) fit the experimental points of azo bioreduction well, irrespectively of the activated carbon used in the bioreactor. According to the $k_1$ kinetic constants achieved for the carbons having different textural properties (Fig. 7), the original sample $AC_0$ presented the smallest decolourisation rates while $AC_{T2}$ with the highest surface area resulted the best azo dye removal. Although the USPBRs with each carbon appeared to be a very effective treatment system, $AC_{T2}$ worked extremely well: conversion values above 88% were achieved in case of both azo dyes at a $\tau$ of 0.23 min or higher corresponding to a very short hydraulic residence time of about 0.30 min at the most (calculated from the reactor hold-up). To the author's knowledge, so far, no better removal rates of azo dyes Orange II and Reactive Black 5 have been reported in anaerobic bioreactors. The Michaelis–Menten constant ($k_2$) was found to be similar in the case of both dyes reduction and of all activated carbons (0.90–0.95 mmol L$^{-1}$).

When plotting $k_1$ constants against the amount of quinonic groups [$CO_Q$] on the referred activated carbon's surface (Fig. 7), two important conclusions can be done. On the one hand, the dye

**Table 3**
Results of the deconvolution of TPD spectra.

| Sample | Carboxylic acid | | Anhydride | | Lactone | | Phenol | | Carbonyl/quinone | |
|---|---|---|---|---|---|---|---|---|---|---|
| | $T_M$ (°C) | $A$ (μmol g$^{-1}$) | $T_M$ (°C) | $A$ (μmol g$^{-1}$) | $T_M$ (°C) | $A$ (μmol g$^{-1}$) | $T_M$ (°C) | $A$ (μmol g$^{-1}$) | $T_M$ (°C) | $A$ (μmol g$^{-1}$) |
| $AC_0$ | 274 | 75 | 575 | 42 | 853 | 17 | 594 | 227 | 931 | 688 |
| $AC_{T0}$ | – | – | 625 | 38 | 810 | 24 | 712 | 226 | 874 | 735 |
| $AC_{T1}$ | – | – | 618 | 41 | 809 | 27 | 706 | 243 | 860 | 811 |
| $AC_{T2}$ | – | – | 617 | 51 | 789 | 41 | 680 | 390 | 856 | 945 |
| $AC_1$ | 299 | 211 | 577 | 159 | 817 | 48 | 677 | 713 | 890 | 1141 |
| $AC_2$ | – | – | 575 | 128 | 775 | 49 | 689 | 632 | 884 | 1019 |
| $AC_3$ | – | – | – | – | 747 | 52 | 743 | 549 | 898 | 886 |
| $AC_4$ | – | – | – | – | 908 | 35 | 667 | 94 | 923 | 780 |
| $AC_5$ | – | – | – | – | – | – | 786 | 27 | 978 | 86 |
| $AC_{02}$ | – | – | – | – | – | – | 786 | 151 | 931 | 347 |

reduction rate is proportional to the activated carbon surface area. This is evidenced when considering the data of $AC_{T0}$, $AC_{T1}$ and $AC_{T2}$, which have similar specific surface chemistries (referred to the $[CO_Q]/S_{BET}$ ratios), since the amount of CO released is directly proportional to the BET surface area. On the other hand, the increase of the amount of CO-releasing groups – mostly, quinonic groups – on the activated carbon surface results higher decolourisation rates, at least, in the given range of $[CO_Q]$. The samples $AC_0$ and $AC_{T0}$ have similar textural properties with nearly the same BET surface areas. However, they slightly differ in surface chemistries and $AC_{T0}$, possessing a denser quinonic surface structure, gave significantly better reduction rates than $AC_0$ for both azo colourants. This confirms the hypothesis of quinonic catalysis in anaerobic azo dye reduction.

### 3.2.3. Catalytic reduction by ACs with different surface chemistries

Comparing to textural modification, variation of the carbon surface groups ($AC_1$–$AC_5$ and $AC_{02}$) seems to have less effect on dye reduction (Fig. 8). Although different surface chemistries were obtained on $AC_1$, $AC_2$, and $AC_3$, they did not present significant differences in azo dye reduction rates, probably due to their similar high carbonyl/quinonic groups surface densities (890–1140 μmol $g_{AC}^{-1}$). It is interesting to note that once the carbon surface chemistry is different, then the accessibility of the dye molecules to the pores and their interaction with the activated carbon surface are expected to be different as well, which may have a certain influence on the dye reduction. On the other hand, the decrease of quinonic groups down to smaller amounts

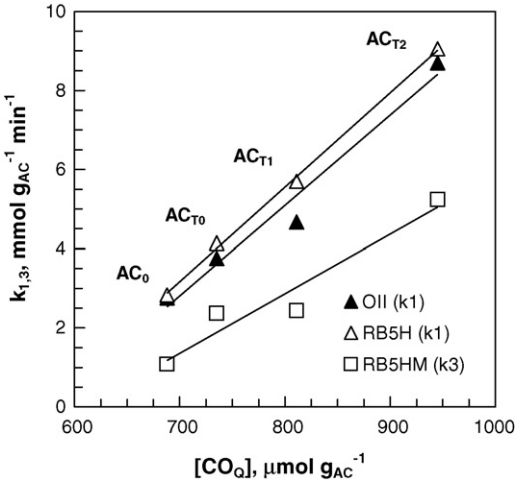


**Fig. 7.** Correlation between catalytic azo reduction and surface quinonic densities of activated carbons with different textural properties.

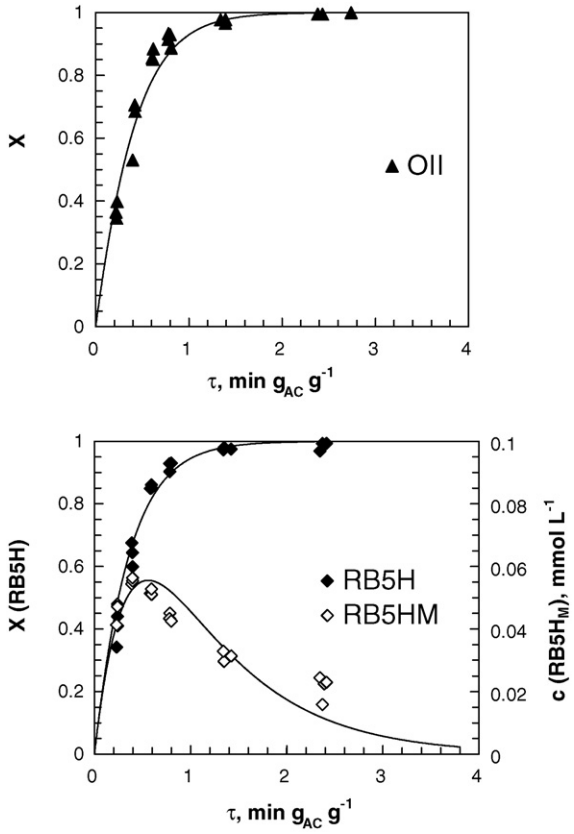


**Fig. 6.** Example of kinetic modeling of azo anaerobic biodecolourisation in USPBR ($AC_0$); lines show the model fitting to experimental points.

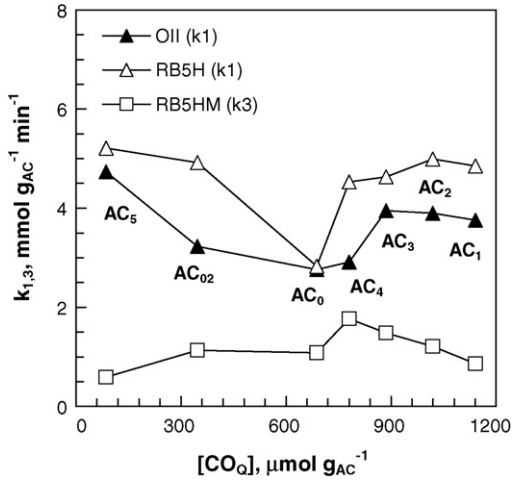


**Fig. 8.** Correlation between catalytic azo reduction and surface quinonic densities of activated carbons with different surface chemistries.

($\sim 600\,\mu mol\,g_{AC}^{-1}$) implied reduction of the catalytic activity of activated carbon. This means that a [$CO_Q$] interval exists where quinonic catalysis of azo reduction occurs. Besides the present anaerobic azo reduction process, carbonyl/quinonic groups on AC surface has also been reported as the decisive sites in different applications such as in the oxidative dehydrogenation of ethylbenzene [29,34] or in electrical double layer capacitors [35]. The $k_2$ constants were found to be between 0.90 and 0.94 mmol $L^{-1}$ for all carbons.

The sample $AC_5$ presented the highest azo dye reduction rates and this performance needs some explanation. Dye adsorption studies for the activated carbon samples ($AC_1$–$AC_5$) were previously done (data not shown) and no significant difference among adsorption capacities of these ACs was found. This confirms the importance of another factor in the reduction process. The thermal treatment at 1100 °C (sample $AC_5$) resulted only a minimal amount of carbonyl groups on the carbon surface. The density of the delocalized π-electrons on the graphene sheets increases upon the removal of the electronegative surface oxygen groups and hence the electrical conductivity increases [36]. Therefore $AC_5$ should have a higher conductivity than the samples $AC_1$–$AC_4$ and $AC_5$ is probably the only sample where the π-electrons extensively participate in the reduction process. Considering all the activated carbon samples with different surface chemistries, their performance in dye decolourisation is probably related to two different reaction mechanisms occurring in the presence/absence of surface oxygen groups: one involves the delocalized π-electrons ($AC_5$ and $AC_{02}$) and the other the surface quinonic functionalities ($AC_1$–$AC_4$). The double mechanism is better surmised when looking the reduction trend of Orange II than of the more biodegradable Reactive Black.

It is interesting to mention that in case of each activated carbon, the hydrolysed reactive dye presented better biodegradability than Orange II. This result is reasonable if considering the electrochemical characteristic of these two dyes. An earlier work of the authors [21] stated that the key factor of azo reduction was not the activated carbon high adsorption capacity for different dyes but the reduction potential value of the colourants. According to these values, the first azo bond reduction in RB5H takes place easier than the anaerobic decolourisation of the monoazo OII, irrespectively of the bioreactor system or the type of activated carbon used as a catalyst.

## 4. Conclusions

Anaerobic decolourisation of two commercially important textile azo dyes was studied in terms of activated carbon modification in upflow stirred packed-bed reactors containing biological activated carbon system. Carbons with different textural properties and various surface chemistries were prepared in order to examine their possible influence on azo dye reduction rates. Characterization of the carbon samples proved that the texturally modified ACs did not differ significantly in surface chemistries and, inversely, surface chemistry modification of ACs by acid- and thermal treatments took place with no significant textural changes. The proposed kinetic model described well the anaerobic catalytic azo reduction for all the activated carbons tested. The azo dye decolourisation rate constants were found to be proportional to the activated carbon surface area. Although variation of the AC surface chemistry seems to have less effect on dye removal rates than the textural properties, the hypothesis of catalysis by carbonyl/quinone sites in the anaerobic dye reduction process was confirmed. An other mechanism plays an important role in the catalytic decolourisation, particularly in the absence of significant densities of surface oxygen-containing groups, when not the quinonic groups but rather the delocalized π-electrons are involved in the reduction. Although the USPBR appears to be a very effective system for biological azo dye treatment with all the activated carbons studied, its performance can be further enhanced by appropriate tailoring of the textural and surface chemistry properties of the catalyst.

## Acknowledgements

The authors gratefully acknowledge the fellowship from Universitat Rovira i Virgili, the financial support provided by the Spanish Ministry of Science and Education (CTM2008-03338) and by the Catalan government (2007ITT-00008). Gergo Mezohegyi, Dr. Azael Fabregat, Dr. Agustí Fortuny, Dr. Josep Font, Dr. Christophe Bengoa and Dr. Frank Stuber are members of the CREPI group (Grup de Recerca Consolidat de la Generalitat de Catalunya, SGR05-00792).

## References

[1] S.H. Lin, M.L. Chen, Water Res. 31 (1997) 868–876.
[2] F.P. van der Zee, R.H.M. Bouwman, D.P.B.T.B. Strik, G. Lettinga, J.A. Field, Biotechnol. Bioeng. 75 (2001) 691–701.
[3] K.T. Chung, S.E.J. Stevens, Environ. Toxicol. Chem. 12 (1993) 2121–2132.
[4] J.H. Weisburger, Mutat. Res. 506 (2002) 9–20.
[5] D.P. Oliveira, P.A. Carneiro, M.K. Sakagami, M.V.B. Zanoni, G.A. Umbuzeiro, Mutat. Res. 626 (2007) 135–142.
[6] E. Forgacs, T. Cserháti, Gy. Oros, Environ. Int. 30 (2004) 953–971.
[7] T. Robinson, G. McMullan, R. Marchant, P. Nigam, Bioresour. Technol. 77 (2001) 247–255.
[8] F.P. van der Zee, S. Villaverde, Water Res. 39 (2005) 1425–1440.
[9] P.C. Vandevivere, R. Bianchi, W. Verstraete, J. Chem. Technol. Biotechnol. 72 (1998) 289–302.
[10] I.M. Banat, P. Nigam, D. Singh, R. Marchant, Bioresour. Technol. 58 (1996) 217–227.
[11] C.I. Pearce, J.R. Lloyd, J.T. Guthrie, Dyes Pigments 58 (2003) 179–196.
[12] A. Stolz, Appl. Microbiol. Biotechnol. 56 (2001) 69–80.
[13] H.-J. Knackmuss, J. Biotechnol. 51 (1996) 287–295.
[14] M. Işık, D.T. Sponza, Enzyme Microbiol. Technol. 38 (2006) 887–892.
[15] C. O'Neill, F.R. Hawkes, D.L. Hawkes, S. Esteves, S.J. Wilcox, Water Res. 34 (2000) 2355–2361.
[16] A.B. dos Santos, I.A.E. Bisschops, F.J. Cervantes, J.B. van Lier, Chemosphere 55 (2004) 1149–1157.
[17] J. Rau, H.-J. Knackmuss, A. Stolz, Environ. Sci. Technol. 36 (2002) 1497–1504.
[18] F.P. van der Zee, I.A.E. Bisschops, G. Lettinga, J.A. Field, Environ. Sci. Technol. 37 (2003) 402–408.
[19] G. Mezohegyi, A. Kolodkin, U.I. Castro, C. Bengoa, F. Stuber, J. Font, A. Fabregat, A. Fortuny, Ind. Eng. Chem. Res. 46 (2007) 6788–6792.
[20] G. Mezohegyi, C. Bengoa, F. Stuber, J. Font, A. Fabregat, A. Fortuny, Chem. Eng. J. 143 (2008) 293–298.
[21] G. Mezohegyi, A. Fabregat, J. Font, C. Bengoa, F. Stuber, A. Fortuny, Ind. Eng. Chem. Res. 48 (2009) 7054–7059.
[22] J.L. Figueiredo, M.F.R. Pereira, in: P. Serp, J.L. Figueiredo (Eds.), Carbon Materials for Catalysis, John Wiley & Sons, Inc., Hoboken, NJ, 2009, pp. 177–217.
[23] L.R. Radovic, F. Rodríguez-Reinoso, in: P.A. Thrower (Ed.), Chemistry and Physics of Carbon, vol. 25, Marcel Dekker, New York, 1997, pp. 243–358.
[24] A. Fortuny, J. Font, A. Fabregat, Appl. Catal. B 19 (1998) 165–173.
[25] J. Rivera-Utrilla, M. Sánchez-Polo, Appl. Catal. B 39 (2002) 319–329.
[26] M.E. Suarez-Ojeda, F. Stüber, A. Fortuny, A. Fabregat, J. Carrera, J. Font, Appl. Catal. B 58 (2005) 105–114.
[27] M.F.R. Pereira, J.J.M. Órfão, J.L. Figueiredo, Colloids Surf. A: Physicochem. Eng. Aspects 241 (2004) 165–171.
[28] J.L. Figueiredo, M.F.R. Pereira, M.M.A. Freitas, J.J.M. Órfão, Carbon 37 (1999) 1379–1389.
[29] M.F.R. Pereira, J.J.M. Órfão, J.L. Figueiredo, Appl. Catal. A 184 (1999) 153–160.
[30] F. Rodriguez-Reinoso, J.M. Martin-Martinez, C. Prado-Burguete, B. McEnaney, J. Phys. Chem. 91 (1987) 515–516.
[31] J.J.M. Órfão, A.I.M. Silva, J.C.V. Pereira, S.A. Barata, I.M. Fonseca, P.C.C. Faria, M.F.R. Pereira, J. Colloid Interface Sci. 296 (2006) 480–489.
[32] J.L. Figueiredo, M.F.R. Pereira, M.M.A. Freitas, J.J.M. Órfão, Ind. Eng. Chem. Res. 46 (2007) 4110–4115.
[33] P.C.C. Faria, J.J.M. Órfão, M.F.R. Pereira, Water Res. 38 (2004) 2043–2052.
[34] J.A. Maciá-Agulló, D. Cazorla-Amorós, A. Linares-Solano, U. Wild, D.S. Su, R. Schlögl, Catal. Today 102–103 (2005) 248–253.
[35] M.J. Bleda-Martínez, J.A. Maciá-Agulló, D. Lozano-Castelló, E. Morallón, D. Cazorla-Amorós, A. Linares-Solano, Carbon 43 (2005) 2677–2684.
[36] D. Pantea, H. Darmstadt, S. Kaliaguine, L. Sümmchen, C. Roy, Carbon 39 (2001) 1147–1158.